

RESEARCH NOTE

Open Access



Uniformly convergent extended cubic B-spline collocation method for two parameters singularly perturbed time-delayed convection-diffusion problems

Naol Tufa Negero^{1*}

Abstract

This work proposes a uniformly convergent numerical scheme to solve singularly perturbed parabolic problems of large time delay with two small parameters. The approach uses implicit Euler and the exponentially fitted extended cubic B-spline for time and space derivatives respectively. Extended cubic B-splines have advantages over classical B-splines. This is because for a given value of the free parameter λ the solution obtained by the extended B-spline is better than the solution obtained by the classical B-spline. To confirm the correspondence of the numerical methods with the theoretical results, numerical examples are presented. The present numerical technique converges uniformly, leading to the current study of being more efficient.

Keywords Singular perturbations, Two parameter convection-diffusion problem, Time delay, Exponentially fitted method, Extended cubic B-spline, Boundary layer

Mathematics Subject Classification 65M06, 65M12, 65L11

Introduction

Consider the two-parameter singularly perturbed one-dimensional parabolic time delay convection-diffusion initial-boundary value problem defined as

$$\begin{cases} \left(\frac{\partial}{\partial t} + L_{\varepsilon, \mu} \right) u(x, t) = H(x, t), (x, t) \in D \\ u(x, t) = \phi_b(x, t), (x, t) \in \Gamma_b = [0, 1] \times [-\tau, 0], \\ u(0, t) = \phi_l(t), \Gamma_l = \{(0, t) : 0 \leq t \leq T\}, \\ u(1, t) = \phi_r(t), \Gamma_r = \{(1, t) : 0 \leq t \leq T\}. \end{cases} \quad (1)$$

where $D = \Omega_x \times (0, T], \Omega_x = (0, 1), 0 < \varepsilon \leq 1, 0 \leq \mu \leq 1, H(x, t) = c(x, t)u(x, t - \tau) + f(x, t)$ and $\tau > 0$ represents the delay parameter and $a(x, t), b(x, t), c(x, t), f(x, t), \phi_b(x, t), \phi_l(t)$ and $\phi_r(t)$ are sufficiently smooth, bounded functions on $\bar{D} = [0, 1] \times [0, T]$, that satisfy

$$a(x, t) \geq \alpha > 0, b(x, t) \geq \beta > 0, c(x, t) \geq \vartheta > 0, \gamma = \min \left(\frac{b}{a} \right).$$

The operator $L_{\varepsilon, \mu}$ given as

$$L_{\varepsilon, \mu} u(x, t) \equiv -\varepsilon u_{xx} - \mu a(x, t) u_x + b(x, t) u.$$

The existence of function approximations has been the subject of extensive research [1–14]. Here, the existence and uniqueness of a solution of (1) can be established under the assumption that the data are Holder continuous and sufficient smoothness of initial-boundary data on $\Gamma = \Gamma_b \cup \Gamma_l \cup \Gamma_r$ and compatibility conditions at the

*Correspondence:

Naol Tufa Negero
 naolt@wollegauniversity.edu.et; natitfa@gmail.com

¹ Department of Mathematics, Wollega University, 395 Nekemte, Oromia, Ethiopia



corner points $(0, 0), (1, 0), (0, -\tau)$ and $(1, -\tau)$, and delay terms [15].

$$\begin{cases} \phi_b(0, 0) = \phi_l(0), \\ \phi_b(1, 0) = \phi_r(0), \end{cases} \quad (2)$$

so that a unique solution exists and is sufficiently smooth for the model problem (1). For $\varepsilon \rightarrow 0$ and $\mu = 1$, numerical methods available in [16, 17] for the problem given by Eqs.(1) whose solution exhibits an exponential boundary layer of width $O(\varepsilon)$ in the left boundary layer Γ_l . As the parameters $\varepsilon \rightarrow 0$ and $\mu \rightarrow 0$, the solution develops boundary layers at $x = 0$ and $x = 1$. The parameters and the ratio ε/μ^2 affect the boundary layer's width. We look at Eq. (1) above with $\varepsilon/\mu^2 \rightarrow 0$ as $\mu \rightarrow 0$ and $\mu^2/\varepsilon \rightarrow 0$ as $\varepsilon \rightarrow 0$. As a result, the uniformly convergent numerical treatment presented in this study is independent of the two parameters ε and μ .

Two-parameter time delayed singularly perturbed parabolic problems have not been studied as extensively as one-parameter problems. Such type of problems are widespread in many phenomena of real life problems (see, for example, [18–20]) described by boundary layer problems. For singularly perturbed one-parameter partial differential equations many works have been delivered numerically in recent years (see, for example, [16, 21–33]). Not much numerical investigations have been done on two-parameter time delayed singularly perturbed parabolic problems. The work on two-parameter time delayed singularly perturbed parabolic problems have been started by Govindarao *et al.* [34], where they considered an upwind difference scheme on the Shishkin type meshes. First-order in both space and time numerical method was established. Sumit *et al.* [35] extend the works, where they considered a hybrid scheme for space consisting of central difference, upwind and midpoint operators on layer adapted piecewise uniform Shishkin mesh. Almost second-order in space and first order in time numerical method was established. Negero [36–40] also considered the problem similar to Sumit *et al.* and proposed numerical methods based on fitted operator methods on a uniform mesh, which improved the rate of convergence. However, for the problem under study, there are no known fitted extended cubic B-spline numerical methods. Here, the paper focus on exponentially fitted extended cubic B-spline for spatial discretization and the implicit Euler method for time discretization on uniform meshes. This is the more accurate compared to existing methods for the problem addressed in this work.

The paper is arranged as follows. Section 2 presents the bounds on the derivatives and exact solution of Eq.

(1). The discrete scheme are discussed in Sect. 3. Section 4 deals with convergence and stability of the proposed numerical scheme. Numerical results are given in Sect. 5 to illustrate the theory. The paper concludes with a discussion of the results obtained.

Notations: In this paper, we denote a generic positive constant by C , independent of mesh parameters μ and ε . The supremum norm on a domain D is defined as

$$\|\tilde{h}\|_{\bar{D}} = \sup_{(x,t) \in \bar{D}} |\tilde{h}(x, t)|.$$

Preliminaries

Lemma 1 (Continuous maximum principle) *Let $z(x, t) \in C^2(D) \cap C^0(\bar{D})$, and assume that $z(x, t) \geq 0, \forall(x, t) \in \Gamma = \Gamma_l \cup \Gamma_b \cup \Gamma_r$. Then $(\frac{\partial}{\partial t} + L_{\varepsilon, \mu})z(x, t) \geq 0$ in D implies that $z(x, t) \geq 0, \forall(x, t) \in \bar{D}$.*

Proof Let $(\zeta^*, \vartheta^*) \in D$ such that $\mathbf{z}(\zeta^*, \vartheta^*) = \min_{(x,t) \in \bar{D}} \mathbf{z}(x, t) < 0$. Then $(\xi^*, \vartheta^*) \notin \Gamma$. Since at the point (ξ^*, ϑ^*) function π attains minimum, then, we have $z_x = z_t = 0$ at (ζ^*, ϑ^*) and $z_{xx}(\zeta^*, \vartheta^*) \geq 0$ and thus,

$$\begin{aligned} \left(\frac{\partial}{\partial t} + L_{\varepsilon, \mu}\right)z(\zeta^*, \vartheta^*) &= \frac{\partial z(\zeta^*, \vartheta^*)}{\partial t} - \varepsilon \frac{\partial^2 z(\zeta^*, \vartheta^*)}{\partial x^2} \\ &\quad - \mu a(\zeta^*, \vartheta^*) \frac{\partial z(\zeta^*, \vartheta^*)}{\partial x} + b(x, t)z(\zeta^*, \vartheta^*) < 0, \end{aligned}$$

which is a contradiction. This implies $z(x, t) \geq 0 \forall(x, t) \in \bar{D}$. \square

Lemma 2 [35] *Let $u(x, t)$ be the solution of problems (1) and i, j are any non-negative integers satisfying $0 \leq i + 3j \leq 4$. Then,*

$$\left\| \frac{\partial^{i+j} u}{\partial x^i \partial t^j} \right\|_{\bar{D}} \leq C \begin{cases} \frac{1}{(\sqrt{\varepsilon})^i}, \text{ if } \frac{\mu^2}{\varepsilon} \rightarrow 0 \text{ as } \varepsilon \rightarrow 0, \\ \left(\frac{\mu}{\varepsilon}\right)^i \left(\frac{\mu^2}{\varepsilon}\right)^j, \text{ if } \frac{\varepsilon}{\mu^2} \rightarrow 0 \text{ as } \mu \rightarrow 0, \end{cases}$$

where C a positive constant independent of the parameters ε and μ .

Discretization of the problem

The time semi-discretization

For the time domain $[0, T]$ equidistant mesh discretization with uniform step size Δt is used such that

$$\Omega_t^M = \{t_m = m\Delta t, m = 0, 1, \dots, M, \Delta t = T/M\},$$

where M is mesh elements used on the interval $[0, T]$. The mesh for $[-\tau, T]$ is defined as

$$\Omega_t^s = \{t_m = m\Delta t, m = 0, 1, \dots, s, t_s = \tau, \Delta t = \tau/s\}.$$

where s mesh elements used on the interval $[-\tau, 0]$. Here, semi-discretizing the given problems (1) by applying implicit Euler scheme written as

$$\begin{cases} \frac{U^m(x) - U^{m-1}(x)}{\Delta t} - \varepsilon(U_{xx})^m(x) - \mu a^m(x)(U_x)^m(x) + b^m(x)U^m(x) \\ = H^m(x), \\ U^m(0) = \phi_l(t_m), 0 \leq m \leq M, x \in \Omega_x, \\ U^m(1) = \phi_r(t_m), 0 \leq m \leq M, x \in \Omega_x, \\ U^m(x) = \phi_b(x, t_m), -s \leq m \leq -1, x \in \Omega_x, \end{cases} \tag{3}$$

where $H^m(x) = -c^m(x)U^{m-s}(x) + f^m(x)$, $0 \leq m \leq M, x \in \Omega_x$ and $U^m(x)$ is the approximate solution of $u(x, t_m)$ at (m) th time level. The Eq. (3) can be rewritten as

$$\begin{cases} (1 + \Delta t L_{\varepsilon, \mu}^{\Delta t})U^m(x) = H(x, t_m), \\ U^m(0) = \phi_l(t_m), m = 0, \dots, M, \\ U^m(1) = \phi_r(t_m), m = 0, \dots, M, \\ U^m(x) = \phi_b(x, t_m), x \in (0, 1), -(s + 1) \leq m \leq -1, \end{cases} \tag{4}$$

where

$$\begin{aligned} L_{\varepsilon, \mu}^{\Delta t} &= -\varepsilon(U_{xx})^m(x) - \mu a^m(x)(U_x)^m(x) + b^m(x)U^m(x) \\ H(x, t_m) &= -\Delta t c^m(x)U^{m-s}(x) + \Delta t f^m(x) + U^m(x). \end{aligned}$$

Lemma 3 (Semi-discrete maximum principle) *Assume that $\Pi^{m+1}(x) \in C^{2,1}(\bar{D})$ such that $\Pi^{m+1}(0) \geq 0$ and $\Pi^{m+1}(1) \geq 0$. Then, $(1 + \Delta t L_{\varepsilon, \mu}^{\Delta t})\Pi^{m+1}(x) \geq 0, \forall x \in D$, implies that $\Pi^{m+1}(x) \geq 0, \forall x \in \bar{D}$.*

Proof Assume $y^* \in \bar{D}$ such that $\Pi^{m+1}(y^*) = \min_{(x) \in \bar{D}} \Pi^{m+1}(x)$ and suppose $\Pi^{m+1}(y^*) < 0$. Now, it is clear that $y^* \notin \{0, 1\}$, which implies that $y^* \in (0, 1)$. Therefore, we have $\frac{d}{dx}(\Pi^{m+1}(y^*)) = 0$ and $\frac{d^2}{dx^2}(\Pi^{m+1}(y^*)) \geq 0$ and thus

$$\begin{aligned} (1 + \Delta t L_{\varepsilon, \mu}^{\Delta t})\Pi^{m+1}(y^*) &= -\varepsilon \Delta t \frac{d^2}{dx^2}(\Pi^{m+1}(y^*)) \\ - \mu \Delta t a^{m+1}(y^*) \frac{d}{dx} \Pi^{m+1}(y^*) &+ (1 + \Delta t)\Pi^{m+1}(y^*) < 0, \end{aligned}$$

this contradicts assumption and $\Pi^{m+1}(y^*) \geq 0$, which implies that $\Pi^{m+1}(x) \geq 0, \forall (x) \in \bar{D}$. \square

Let $u(x, t_m)$ be the exact and $U^m(x)$ be the approximate solution of the problem in (1). The error estimates for the temporal semi-discretization (4) $E_{m+1} = U^m(x) - u(x, t_m)$ satisfy the following Lemma.

Lemma 4 (Local error estimate) *The local error estimate with the semi-discretized problem (4) is given by*

$$\|E_{m+1}\|_{\infty} \leq C(\Delta t)^2.$$

Proof Applying Taylor’s series expansion to $u(x, t_m)$ gives,

$$u(x, t_{m+1}) = u(x, t_m) + \Delta t u_t(x, t_m) + O((\Delta t)^2). \tag{5}$$

Substituting (5) into the continuous problems (1) gives,

$$\begin{aligned} \frac{u(x, t_{m+1}) - u(x, t_m)}{\Delta t} &= u_t(x, t_m) + O((\Delta t)^2) \\ &= \varepsilon u_{xx}(x, t_{m+1}) + \mu a(x, t_{m+1})u_x(x, t_{m+1}) \\ &\quad - b(x, t_{m+1})u(x, t_{m+1}) - c(x, t_{m+1})u(x, t_{-s+m}) \\ &\quad + f(x, t_{m+1}) \\ &\quad + O((\Delta t)^2). \end{aligned}$$

Clearly $E_{m+1}(x)$ satisfies the semi-discrete operator

$$(1 + \Delta t L_{\varepsilon, \mu}^{\Delta t})E_{m+1}(x) = O((\Delta t)^2),$$

with the conditions:

$$E_{m+1}(0) = E_{m+1}(1) = 0.$$

Thus using maximum principle given at Lemma 3 we have

$$\|E_{m+1}\|_\infty \leq C(\Delta t)^2.$$

□

Lemma 5 (Global error estimate.) *The global error estimate TE_m in the temporal direction at t_m is given by*

$$\|TE_m\| \leq C(\Delta t).$$

Proof The global error estimate at the (m) th time step is given by

$$\begin{aligned} \|TE_m\|_\infty &= \left\| \sum_{k=1}^m e_k \right\|_\infty, m \leq \frac{T}{\Delta t} \\ &\leq \|e_1\|_\infty + \|e_2\|_\infty + \dots + \|e_m\|_\infty. \end{aligned}$$

Using local error estimates given in Lemma 4,

$$\begin{aligned} &\leq C_1((m)\Delta t)(\Delta t) \\ &\leq C_1T(\Delta t), \text{ since } m(\Delta t) \leq T \\ &\leq C(\Delta t), C = C_1T, \end{aligned}$$

where C is constant independent of ε, μ and Δt . □

Lemma 6 [41] *The solution $U^m(x)$ of semi-discretized scheme (4) and its derivatives satisfies*

$$\begin{aligned} \left| \frac{d^i U^m(x)}{dx^i} \right| &\leq C \left(1 + \omega_1^{-i} e^{-\nu\omega_1 x} + \omega_2^{-i} e^{-\nu\omega_2(1-x)} \right), \\ &\text{for } 0 \leq i \leq 4, \end{aligned}$$

where ν is any real constant number, $\lambda_1(x)$ and $\lambda_2(x)$ are two real solutions of (4) such that $\lambda_1(x) < 0$ and $\lambda_2(x) > 0$ and by assumption $\omega_1 = -\max_{x \in [0,1]} \lambda_1(x)$ and $\omega_2 = \min_{x \in [0,1]} \lambda_2(x)$.

Discrete extended cubic B-splines construction

The spatial domain $[0, 1]$ is discretized into N equal number of mesh elements each of length $h = N^{-1}$. This gives the spatial mesh

$$\Omega_x^N = \{x_n = nh, n = 1, 2, \dots, N, x_0 = 0, x_N = 1\},$$

where x_n is mesh points. The extended cubic B-spline basis of degree 4, $K_n(x, \lambda)$, is defined as the form

$$\begin{aligned} K_n(x, \lambda) &= \frac{1}{24h^4} \begin{cases} 4h(1-\lambda)(x-x_{n-2})^3 + 3\lambda(x-x_{n-2})^4, x \in [x_{n-2}, x_{n-1}], \\ (4-\lambda)h^4 + 12h^3(x-x_{n-1}) \\ + 6h^2(2+\lambda)(x-x_{n-1})^2 - 12h(x-x_{n-1})^3 \\ - 3\lambda(x-x_{n-1})^4, x \in [x_{n-1}, x_n], \\ (4-\lambda)h^4 + 12h^3(x_{n+1}-x) \\ + 6h^2(2+\lambda)(x_{n+1}-x)^2 - 12h(x_{n+1}-x)^3 \\ - 3\lambda(x_{n+1}-x)^4, x \in [x_n, x_{n+1}], \\ 4h(1-\lambda)(x_{n+2}-x)^3 + 3\lambda(x_{n+2}-x)^4, x \in [x_{n+1}, x_{n+2}], \\ 0, \text{ otherwise.} \end{cases} \end{aligned} \tag{6}$$

An approximation extended cubic B-spline function, $S(x, \lambda)$ to the exact solution $U(x, t_{m+1})$ at $(m + 1)$ th time level is a linear combination of the extended cubic B-spline basis as

$$S(x, \lambda) = \sum_{n=-1}^{N+1} \zeta_n K_n(x, \lambda), \tag{7}$$

where ζ_n 's are coefficients to be determined by collocation at each time level. Using the approximation given by (7) and Table 1 at nodal points $x = x_m$ in (4) gives, The Eq. (3) can be rewritten as

$$\begin{cases} (1 + \Delta t L_{\varepsilon, \mu}^{\Delta t, h}) U^{m+1}(x_n) = H(x_n, t_m), \\ U^{m+1}(0) = \phi_l(t_{m+1}), m = 0, \dots, M, \\ U^{m+1}(1) = \phi_r(t_{m+1}), m = 0, \dots, M, \\ U^{m+1}(x_n) = \phi_b(x_n, t_{m+1}), x_n \in (0, 1), -(s+1) \leq m \leq -1, \end{cases} \tag{8}$$

where

$$\begin{aligned} L_{\varepsilon, \mu}^{\Delta t, h} &= -\sigma(\varepsilon, \mu)(U_{xx})^{m+1}(x_n) \\ &\quad - \mu a^{m+1}(x_n)(U_x)^{m+1}(x_n) \\ &\quad + b^{m+1}(x_n)U^{m+1}(x_n), \\ H(x_n, t_m) &= -\Delta t c^{m+1}(x_n)U^{m+1-s}(x_n) \\ &\quad + \Delta t f^{m+1}(x_n) + U^m(x_n). \end{aligned}$$

Putting the approximation (7) into collocation (8) the operator $1 + \Delta t L_{\varepsilon, \mu}^{\Delta t, h}$ in (8) is given as

Table 1 Values of $K_n(x)$ and its first two derivatives at the nodal points

x	x_{n-1}	x_n	x_{n+1}	Otherwise
$K_n(x, \lambda)$	$\frac{4-\lambda}{24}$	$\frac{8+\lambda}{12}$	$\frac{4-\lambda}{24}$	0
$K'_n(x, \lambda)$	$\frac{-1}{2h}$	0	$\frac{1}{2h}$	0
$K''_n(x, \lambda)$	$\frac{2+\lambda}{2h^2}$	$-\frac{2+\lambda}{h^2}$	$\frac{2+\lambda}{2h^2}$	0

$$r_n^- \zeta_{n-1} + r_n^c \zeta_n + r_n^+ \zeta_{n+1} = H(x_n, t_m), 0 \leq n \leq N, \tag{9}$$

where

$$\begin{cases} r_n^- = -\sigma(\varepsilon, \mu)\Delta t \frac{2+\lambda}{2h^2} + \mu\Delta t \frac{1}{2h} a^{m+1}(x_n) + \frac{4-\lambda}{24} (1 + \Delta t b^{m+1}(x_n)), \\ r_n^c = \sigma(\varepsilon, \mu)\Delta t \frac{2+\lambda}{h^2} + \frac{8+\lambda}{12} \Delta t b^{m+1}(x_n), \\ r_n^+ = -\sigma(\varepsilon, \mu)\Delta t \frac{2+\lambda}{2h^2} - \mu\Delta t \frac{1}{2h} a^{m+1}(x_n) + \frac{4-\lambda}{24} (1 + \Delta t b^{m+1}(x_n)), \end{cases}$$

where $\sigma(\varepsilon, \mu) = \varepsilon \frac{\rho \mu a_m}{2+\lambda} \coth\left(\mu \frac{\rho a_m}{2}\right)$.

For the given boundary conditions we have

$$\begin{cases} \frac{4-\lambda}{24} \zeta_{-1} + \frac{8+\lambda}{12} \zeta_0 + \frac{4-\lambda}{24} \zeta_1 = \phi_l(t_{m+1}), \\ \frac{4-\lambda}{24} \zeta_{N-1} + \frac{8+\lambda}{12} \zeta_N + \frac{4-\lambda}{24} \zeta_{N+1} = \phi_r(t_{m+1}). \end{cases} \tag{10}$$

The Eqs.(9)-(10) gives to $(N + 3) \times (N + 3)$ systems in $(N + 3)$ unknowns $\zeta_{-1}, \zeta_0, \zeta_1, \dots, \zeta_{N+1}$. From Eqs. (9)-(10), eliminating ζ_{-1} and ζ_{N+1} results $(N + 1)$ system of equations in $(N + 1)$ unknowns $\zeta_0, \zeta_1, \dots, \zeta_N$ which can be written in a matrix form as

$$RV = Q, \tag{11}$$

where

$$R = \begin{pmatrix} -2\left(\frac{8+\lambda}{4-\lambda}\right)r_0^- + r_0^c & -r_0^- + r_0^+ & 0 & \dots & \dots & \dots & \dots & \dots & 0 \\ R_1(x_1) & R_2(x_1) & R_3(x_1) & 0 & 0 & \dots & \dots & \dots & 0 \\ 0 & R_1(x_2) & R_2(x_2) & R_3(x_3) & 0 & \dots & \dots & \dots & 0 \\ \vdots & \ddots & \ddots & \ddots & \vdots & \vdots & \vdots & \vdots & \vdots \\ 0 & \dots & \dots & \dots & 0 & R_1(x_{N-1}) & R_2(x_{N-1}) & R_3(x_{N-1}) & \\ 0 & \dots & \dots & \dots & \dots & 0 & r_N^- - r_N^+ & r_N^c - 2\left(\frac{8+\lambda}{4-\lambda}\right)r_N^+ & \end{pmatrix},$$

where $R_n(x_n), n = 1, 2, \dots, N - 1$ are defined as

$$\begin{cases} R_1(x_n) = -\sigma(\varepsilon, \mu)\Delta t \frac{2+\lambda}{2h^2} + \mu\Delta t \frac{1}{2h} a^{m+1}(x_n) + \frac{4-\lambda}{24} (1 + \Delta t b^{m+1}(x_n)), \\ R_2(x_n) = \sigma(\varepsilon, \mu)\Delta t \frac{2+\lambda}{h^2} + \frac{8+\lambda}{12} \Delta t b^{m+1}(x_n), \\ R_3(x_n) = -\sigma(\varepsilon, \mu)\Delta t \frac{2+\lambda}{2h^2} - \mu\Delta t \frac{1}{2h} a^{m+1}(x_n) + \frac{4-\lambda}{24} (1 + \Delta t b^{m+1}(x_n)), \end{cases}$$

and column vectors V and Q are given as $V = [\zeta_0, \zeta_1, \dots, \zeta_N]^T$ and

$$Q = \begin{bmatrix} H(x_0, t_m) - \phi_l(t_{m+1})r_0^-, H(x_1, t_m), H(x_2, t_m), \dots, \\ H(x_N, t_m) - \phi_r(t_{m+1})r_N^+ \end{bmatrix}^T.$$

The matrix associated with Eq. (11) is of size $(N + 1) \times (N + 1)$ with its entries for $n = 1, 2, \dots, N - 1$ are $R_1(x_n) < 0, R_2(x_n) > 0, R_3(x_n) < 0$. Therefore, the matrix R in Eq. (11) is an M-matrix and therefore its inverse exist and positive. Hence, tridiagonal system in Eq. (11) easily solved by any existing methods.

Convergence analysis

Lemma 7 *The extended cubic B-splines $K_{-1}(x, \lambda), K_0(x, \lambda), \dots, K_N(x, \lambda), K_{N+1}(x, \lambda)$ satisfy*

$$\sum_{n=-1}^{N+1} |K_n(x, \lambda)| \leq 1.75, 0 < x < 1.$$

Proof At x_n ,

$$\begin{aligned} \sum_{n=-1}^{N+1} |K_n(x, \lambda)| &= |K_{n-1}(x_n, \lambda)| + |K_n(x_n, \lambda)| + |K_{n+1}(x_n, \lambda)| \\ &= \frac{4 - \lambda}{24} + \frac{8 + \lambda}{12} + \frac{4 - \lambda}{24} = 1. \end{aligned}$$

For $x_{n-1} < x < x_{n+1}$,

$$\begin{aligned} |K_n(x, \lambda)| &< \frac{8 + \lambda}{12}, |K_{n-1}(x, \lambda)| < \frac{4 - \lambda}{24}, \\ |K_{n+1}(x, \lambda)| &< \frac{4 - \lambda}{24}, \\ |K_{n-2}(x, \lambda)| &< \frac{4 - \lambda}{24}. \end{aligned}$$

Thus, for $x_{n-1} < x < x_{n+1}$,

$$\begin{aligned} \sum_{n=-1}^{N+1} |K_n(x, \lambda)| &= |K_{n-1}(x_n, \lambda)| + |K_n(x_n, \lambda)| \\ &+ |K_{n+1}(x_n, \lambda)| + |K_{n-2}(x_n, \lambda)| = \frac{20 + \lambda}{12}. \end{aligned}$$

Since $-8 < \lambda < 1$, so $\frac{20+\lambda}{12} \leq 1.75$ and this complete the proof. \square

Theorem 1 Let $u(x_n, t_{m+1})$ be the continuous solution of Eqs. (1) and (2) and $S(x, \lambda)$ be the collocation approximation from the space of splines to the solution $U^{m+1}(x)$ be the approximate solution of Eq. (3). Then, for sufficiently large N , the following error bound holds

$$\begin{aligned} &|L_{\varepsilon, \mu}^{\Delta t, h} U^{m+1}(x_n) - L_{\varepsilon, \mu}^{\Delta t, h} Z_N(x_n)| \\ &= |L_{\varepsilon, \mu}^{\Delta t, h} S(x_n, \lambda) - L_{\varepsilon, \mu}^{\Delta t, h} Z_N(x_n)| \\ &= \left| -\varepsilon \left(\frac{d^2 U^{m+1}(x_n)}{dx^2} - \sigma(\varepsilon, \mu) \frac{d^2 Z_N(x_n)}{dx^2} \right) \right. \\ &\quad \left. + |-\mu a(x) \left(\frac{dU^{m+1}(x_n)}{dx} - \frac{dZ_N(x_n)}{dx} \right) + b^{m+1}(x) (U^{m+1}(x_n) - Z_N(x_n))| \right. \\ &\leq |\varepsilon| |\sigma(\varepsilon, \mu)| \left\| \frac{d^2 U^{m+1}(x_n)}{dx^2} \right\|_{\infty} + |\varepsilon| |\sigma(\varepsilon, \mu)| \left\| \frac{d^2 U^{m+1}(x_n)}{dx^2} - \frac{d^2 Z_N(x_n)}{dx^2} \right\|_{\infty} \\ &\quad + |\mu| \|a(x)\|_{\infty} \left\| \frac{dU^{m+1}(x_n)}{dx} - \frac{dZ_N(x_n)}{dx} \right\|_{\infty} + \|b^{m+1}(x)\|_{\infty} \|U^{m+1}(x_n) - Z_N(x_n)\|_{\infty}. \end{aligned} \tag{15}$$

$$|L_{\varepsilon, \mu}^{\Delta t, h} (U^{m+1}(x_n) - S(x_n, \lambda))| \leq CN^{-2}.$$

Proof Let $Z_N(x_n)$ be a unique spline interpolate to the solution $U^{m+1}(x_n)$ of the problem (3) given by

$$Z_N(x_n) = \sum_{n=-1}^{N+1} \bar{\zeta}_n K_n(x, \lambda). \tag{12}$$

The estimates given in [42] yields

$$\begin{aligned} \|U^{m+1}(x_n) - Z_N(x_n)\|_{\infty} &\leq C_0 \left\| \frac{d^4 U^{m+1}(x_n)}{dx^4} \right\|_{\infty} N^{-4} \\ \left\| \frac{dU^{m+1}(x_n)}{dx} - \frac{dZ_N(x_n)}{dx} \right\|_{\infty} &\leq C_1 \left\| \frac{d^4 U^{m+1}(x_n)}{dx^4} \right\|_{\infty} N^{-3} \\ \left\| \frac{d^2 U^{m+1}(x_n)}{dx^2} - \frac{d^2 Z_N(x_n)}{dx^2} \right\|_{\infty} &\leq C_0 \left\| \frac{d^4 U^{m+1}(x_n)}{dx^4} \right\|_{\infty} N^{-2}. \end{aligned} \tag{13}$$

Using triangle inequality,

$$\begin{aligned} \|U^{m+1}(x_n) - S(x_n, \lambda)\|_{\infty} &\leq \|U^{m+1}(x_n) - Z_N(x_n)\|_{\infty} \\ &+ \|Z_N(x_n) - S(x_n, \lambda)\|_{\infty}. \end{aligned} \tag{14}$$

The collocating conditions are $L_{\varepsilon, \mu}^{\Delta t, h} U^{m+1}(x_n) = L_{\varepsilon, \mu}^{\Delta t, h} S(x_n, \lambda) = H(x_n, t_m)$. Assume that $L_{\varepsilon, \mu}^{\Delta t, h} Z_N(x_n) = \bar{H}(x_n, t_m)$ which satisfies the boundary conditions $Z_N(x_1) = Z_N(x_{N+1})$. Then,

Using Lemma 1 and using Eq.(13)

$$\max_{x \in D} |L_{\varepsilon,\mu}^{\Delta t,h} U^{m+1}(x_n) - L_{\varepsilon,\mu}^{\Delta t,h} Z_N(x_n)| \leq CN^{-2},$$

this is because $|\sigma(\varepsilon, \mu) - 1| \leq CN^{-2}$. Equation (11) and $L_{\varepsilon,\mu}^{\Delta t,h} U^{m+1}(x_n) - L_{\varepsilon,\mu}^{\Delta t,h} Z_N(x_n)$ results

$$R(V - \bar{V}) = Q - \bar{Q}, \tag{16}$$

where

$$V - \bar{V} = (\zeta_0 - \bar{\zeta}_0, \zeta_1 - \bar{\zeta}_1, \dots, \zeta_N - \bar{\zeta}_N),$$

$$Q - \bar{Q} = \left(H(x_0, t_m) - \bar{H}(x_0, t_m), H(x_1, t_m) - \bar{H}(x_1, t_m), \dots, H(x_N, t_m) - \bar{H}(x_N, t_m) \right).$$

The matrices R is invertible, i.e., $|R^{-1}| \leq C$, and the boundary conditions are bounded. Therefore, Eqs. (15) and (16) results $|V - \bar{V}| \leq CN^{-2}$. Thus, Eqs. (7) and (12) gives

$$\|S(x_n, \lambda) - Z_N(x)\|_\infty = |\zeta_n - \bar{\zeta}_n| \sum_{n=0}^{N+2} |K_n(x, \lambda)| \leq CN^{-2}.$$

□

Theorem 2 Let $u(x_n, t_{m+1})$ be the solution of the continuous problem (1)-(2) and U_n^{m+1} be the numerical solution of (8). Then, there exists a constant C such that the following uniform error estimate holds:

$$\sup_{0 < \varepsilon \leq 1} \max_{0 \leq n \leq N, 0 \leq m \leq M} |u(x_n, t_{m+1}) - U_n^{m+1}| \leq C(\Delta t + N^{-2}).$$

Proof The proof is the consequence of Lemma 5 and Theorem 1. □

Numerical examples and results

In this section, two numerical results are used to confirm the theoretical results using the proposed numerical scheme. The exact solution of the numerical example is not available. Therefore, double mesh principle is used to find the maximum absolute error $E_{\varepsilon,\mu}^{N,M}$ and the corresponding convergence order $p_{\varepsilon,\mu}^{N,M}$ as

$$E_{\varepsilon,\mu}^{N,M} = \max_{0 \leq n \leq N, 0 \leq m \leq M} |U_n^{m+1} - U_{2n}^{2m+1}| \text{ and } p_{\varepsilon,\mu}^{N,M} = \log_2 \left(\frac{E_{\varepsilon,\mu}^{N,M}}{E_{\varepsilon,\mu}^{2N,2M}} \right).$$

Table 2 $E_{\varepsilon,\mu}^{N,M}$ and $p_{\varepsilon,\mu}^{N,M}$ with $\mu = 10^{-4}, \lambda = -1e - 03$, for Example 1

$\varepsilon \downarrow$	$N = 32$ $\Delta t = 0.25/2$	$N = 64$ $\Delta t = 0.25/2^2$	$N = 128$ $\Delta t = 0.25/2^3$	$N = 256$ $\Delta t = 0.25/2^4$
10^{-0}	5.7908e - 03 0.66626	3.6490e - 03 0.77604	2.1309e - 03 0.87324	1.1633e - 03
10^{-2}	1.0523e - 02 0.94283	5.4742e - 03 0.97042	2.7938e - 03 0.98490	1.4116e - 03
10^{-4}	1.0658e - 02 0.94630	5.5311e - 03 0.97249	2.8188e - 03 0.98615	1.4230e - 03
10^{-6}	1.0662e - 02 0.94650	5.5324e - 03 0.97267	2.8191e - 03 0.98620	1.4231e - 03
10^{-8}	1.0663e - 02 0.94632	5.5336e - 03 0.97252	2.8200e - 03 0.98605	1.4237e - 03
10^{-10}	1.0663e - 02 0.94632	5.5336e - 03 0.97252	2.8200e - 03 0.98605	1.4237e - 03
10^{-12}	1.0663e - 02 0.94632	5.5336e - 03 0.97252	2.8200e - 03 0.98605	1.4237e - 03
$E_{\varepsilon,\mu}^{N,M}$	1.0663e - 02	5.5336e - 03	2.8200e - 03	1.4880e - 03
$p_{\varepsilon,\mu}^{N,M}$	0.94632	0.97252	0.92232	-

Table 3 $E_{\varepsilon,\mu}^{N,M}$ and $p_{\varepsilon,\mu}^{N,M}$ with $\mu = 10^{-4}, \lambda = -1e - 03$, for Example 2

$\varepsilon \downarrow$	$N = 32$ $\Delta t = 0.25/2$	$N = 64$ $\Delta t = 0.25/2^2$	$N = 128$ $\Delta t = 0.25/2^3$	$N = 256$ $\Delta t = 0.25/2^4$
10^{-0}	1.5539e - 04 0.73824	9.3152e - 05 0.87396	5.0828e - 05 0.93816	2.6527e - 05
10^{-2}	2.1188e - 03 0.88023	1.1511e - 03 0.94229	5.9904e - 04 0.97115	3.0557e - 04
10^{-4}	2.6785e - 03 0.88607	1.4493e - 03 0.94345	7.5362e - 04 0.97160	3.8430e - 04
10^{-6}	2.6752e - 03 0.88449	1.4491e - 03 0.94231	7.5411e - 04 0.97040	3.8487e - 04
10^{-8}	2.6752e - 03 0.88469	1.4489e - 03 0.94318	7.5355e - 04 0.97162	3.8426e - 04
10^{-10}	2.6752e - 03 0.88469	1.4489e - 03 0.94318	7.5355e - 04 0.97162	3.8426e - 04
10^{-12}	2.6752e - 03 0.88469	1.4489e - 03 0.94318	7.5355e - 04 0.97162	3.8426e - 04
$E_{\varepsilon,\mu}^{N,M}$	2.6752e - 03	1.4493e - 03	5.9904e - 04	3.8426e - 04
$p_{\varepsilon,\mu}^{N,M}$	0.88429	1.2746	0.64057	-

Table 4 $E_{\varepsilon,\mu}^{N,M}$ and $p_{\varepsilon,\mu}^{N,M}$ with $\lambda = -1e - 03$, for Example 1

$\varepsilon \downarrow \mu \rightarrow$	$N = 32$	$N = 64$	$N = 128$	$N = 256$
	$\Delta t = 0.125/2$	$\Delta t = 0.125/2^2$	$\Delta t = 0.125/2^3$	$\Delta t = 0.125/2^4$
	10^{-4}	10^{-6}	10^{-8}	10^{-10}
10^{-2}	5.5116e - 03 0.97555	2.8029e - 03 0.98744	1.4137e - 03 0.99352	7.1003e - 04
10^{-4}	5.5305e - 03 0.97258	2.8183e - 03 0.98609	1.4228e - 03 0.99302	7.1485e - 04
10^{-6}	5.5341e - 03 0.97357	2.8182e - 03 0.98604	1.4228e - 03 0.99302	7.1485e - 04
10^{-8}	5.5349e - 03 0.97378	2.8182e - 03 0.98604	1.4228e - 03 0.99302	7.1485e - 04
10^{-10}	5.5349e - 03 0.97378	2.8182e - 03 0.98604	1.4228e - 03 0.99302	7.1485e - 04
10^{-12}	5.5349e - 03 0.97378	2.8182e - 03 0.98604	1.4228e - 03 0.99302	7.1485e - 04
$E_{\varepsilon,\mu}^{N,M}$	5.5349e - 03	2.8183e - 03	1.4228e - 03	7.1485e - 04
$p_{\varepsilon,\mu}^{N,M}$	0.97378	0.98604	0.99302	-

Table 5 $E_{\varepsilon,\mu}^{N,M}$ and $p_{\varepsilon,\mu}^{N,M}$ with $\lambda = -1e - 03$, for Example 2

$\varepsilon \downarrow \mu \rightarrow$	$N = 32$	$N = 64$	$N = 128$	$N = 256$
	$\Delta t = 0.125/2$	$\Delta t = 0.125/2^2$	$\Delta t = 0.125/2^3$	$\Delta t = 0.125/2^4$
	10^{-4}	10^{-6}	10^{-8}	10^{-10}
10^{-0}	7.0128e - 05 0.64823	4.4746e - 05 0.84168	2.4968e - 05 0.92458	1.3154e - 05
10^{-2}	1.1458e - 03 0.94041	5.9706e - 04 0.96902	3.0501e - 04 0.98462	1.5414e - 04
10^{-4}	1.4510e - 03 0.94514	7.5362e - 04 0.97209	3.8417e - 04 0.98576	1.9399e - 04
10^{-6}	1.4434e - 03 0.93362	7.5568e - 04 0.97179	3.8530e - 04 0.98592	1.9454e - 04
10^{-8}	1.4434e - 03 0.93366	7.5566e - 04 0.97172	3.8531e - 04 0.98595	1.9454e - 04
10^{-10}	1.4434e - 03 0.93366	7.5566e - 04 0.97172	3.8531e - 04 0.98595	1.9454e - 04
10^{-12}	1.4434e - 03 0.93366	7.5566e - 04 0.97172	3.8531e - 04 0.98595	1.9454e - 04
$E_{\varepsilon,\mu}^{N,M}$	1.1458e - 03	7.5568e - 04	3.8531e - 04	1.9454e - 04
$p_{\varepsilon,\mu}^{N,M}$	0.93366	0.97172	0.98595	-

The uniform error before extrapolation $E^{N,M}$ and the corresponding uniform order of convergence before extrapolation $p^{N,M}$ by:

$$E^{N,M} = \max_{\varepsilon,\mu} E_{\varepsilon,\mu}^{N,M} \text{ and } p^{N,M} = \log_2 \left(\frac{E^{N,M}}{E^{2N,2M}} \right),$$

where U_m^{n+1} is a numerical solution obtained using the space and time $N \times M$ mesh spacing with a mesh size of h or Δt .

Table 6 $E_{\varepsilon,\mu}^{N,M}$ and $p_{\varepsilon,\mu}^{N,M}$ with $\mu = 10^{-3}, \lambda = 0$, for Example 1

$\varepsilon \downarrow$	$N = 32$ $\Delta t = 0.25$	$N = 64$ $\Delta t = 0.25/2^2$	$N = 128$ $\Delta t = 0.25/2^4$	$N = 256$ $\Delta t = 0.25/2^6$
10^{-0}	7.3970e-03 1.0194	3.6490e-03 1.6482	1.1642e-03 1.8969	3.1262e-04
10^{-2}	1.9438e-02 1.8279	5.4750e-03 1.9530	1.4141e-03 1.9879	3.5651e-04
10^{-4}	1.9861e-02 1.8438	5.5330e-03 1.9586	1.4235e-03	3.5849e-04
10^{-6}	1.9905e-02 1.8409	5.5564e-03 1.9526	1.4355e-03 1.9797	3.6396e-04
10^{-8}	1.9905e-02 1.8409	5.5564e-03 1.9526	1.4355e-03 1.9772	3.6459e-04
10^{-10}	1.9905e-02 1.8409	5.5564e-03 1.9526	1.4355e-03 1.9772	3.6459e-04
10^{-12}	1.9905e-02 1.8409	5.5564e-03 1.9526	1.4355e-03 1.9772	3.6459e-04
$E_{\varepsilon,\mu}^{N,M}$	1.9905e-02	5.5564e-03	1.4355e-03	3.6459e-04
Method in [35]				
$E_{\varepsilon,\mu}^{N,M}$	4.3706e-02	7.3807e-03	1.8967e-03	4.7927e-04

Table 7 $E_{\varepsilon,\mu}^{N,M}$ and $p_{\varepsilon,\mu}^{N,M}$ with $\mu = 10^{-9}, \lambda = 0$, for Example 2

$\varepsilon \downarrow$	$N = 32$ $\Delta t = 0.25$	$N = 64$ $\Delta t = 0.25/2^2$	$N = 128$ $\Delta t = 0.25/2^4$	$N = 256$ $\Delta t = 0.25/2^6$
10^{-0}	2.8379e-04 1.6073	9.3145e-05 1.8997	2.4962e-05 1.9749	6.3499e-06
10^{-2}	3.6086e-03 1.6493	1.1504e-03 1.9158	3.0489e-04 1.9791	7.7337e-05
10^{-4}	4.5529e-03 1.6527	1.4480e-03 1.9150	3.8396e-04 1.9785	9.7429e-05
10^{-6}	4.5651e-03 1.6523	1.4523e-03 1.9151	3.8509e-04 1.9788	9.7695e-05
10^{-8}	4.5652e-03 1.6523	1.4523e-03 1.9150	3.8510e-04 1.9788	9.7698e-05
10^{-10}	4.5652e-03 1.6523	1.4523e-03 1.9150	3.8510e-04 1.9788	9.7698e-05
10^{-12}	4.5652e-03 1.6523	1.4523e-03 1.9150	3.8510e-04 1.9788	9.7698e-05
$E_{\varepsilon,\mu}^{N,M}$	4.5652e-03	1.4523e-03	3.8510e-04	9.7698e-05
Method in [35]				
$E_{\varepsilon,\mu}^{N,M}$	1.1100e-02	2.4588e-03	6.0458e-04	1.5049e-04

Example 1 Consider problem

$$\frac{\partial u}{\partial t} - \varepsilon \frac{\partial^2 u}{\partial x^2} - \mu(1+x) \frac{\partial u}{\partial x} + u(x,t) = u(x,t - \tau) - 16x^2(1-x)^2, (x,t) \in (0,1) \times (0,2],$$

with

$$\begin{cases} u(0,t) = 0, u(1,t) = 0, t \in (0,2], \\ u(x,t) = 0, (x,t) \in [0,1] \times [-\tau,0]. \end{cases}$$

Example 2 Consider problem

$$\begin{aligned} \frac{\partial u}{\partial t} - \varepsilon \frac{\partial^2 u}{\partial x^2} - \mu(1+x(1-x)+t^2) \frac{\partial u}{\partial x} + (1+5xt)u(x,t) \\ = u(x,t - \tau) + x(1-x)(e^t - 1), \\ (x,t) \in (0,1) \times (0,2], \end{aligned}$$

with

$$\begin{cases} u(0,t) = 0, u(1,t) = 0, t \in (0,2], \\ u(x,t) = 0, (x,t) \in [0,1] \times [-\tau,0]. \end{cases}$$

Maximum pointwise errors ($E_{\varepsilon,\mu}^{N,M}$) and rate of convergence ($p_{\varepsilon,\mu}^{N,M}$) for Example 1 and Example 2 have been demonstrated by fixing $\mu = 10^{-4}$ and $\lambda = -1e - 03$ in Tables 2, 3 respectively, for various values of ε . The results given in Tables 2, 3 clearly indicate that the proposed numerical method is accurate of order $O((\Delta t) + N^{-2})$.

Also, tabulated results in Tables 4, 5 indicates that maximum point-wise errors going to stabilized as the two parameters μ and ε approaches to zero. Comparisons of our numerical results with those of [35] are presented in Tables 6, 7. From these tables, we can confirm the more accurate of the proposed numerical method. The numerical solutions obtained by the numerical scheme presented in Example 1 are shown in Fig. 1a, b and numerical scheme presented in Example 2 are shown in Fig. 2a, b. From Figs. 1a, 2a, we confirm the occurrence of both left and right boundary layers near $x = 0$ and $x = 1$ for $\mu = 10^{-6}$ and boundary layers near $x = 0$ for $\mu = 10^{-1}$. The graphs between N and maximum pointwise errors of Examples 1 and 2 are plotted as the log-log scale respectively, in Fig. 3a, b. From these two graphs, one can observe that the numerical scheme converges uniformly as the perturbation parameters goes very small.

Conclusion

In this paper, the exponentially fitted strategy is applied to extended cubic B-spline scheme for solving a two-parameter singularly perturbed temporal delay parabolic problem. In our present study of continuous problem, the temporal direction is discretized by an implicit-Euler scheme with a uniform mesh, and the spatial direction is discretized by an exponentially fitted extended cubic B-spline finite difference method fitting only one parameter ε . We have proved that the method provides

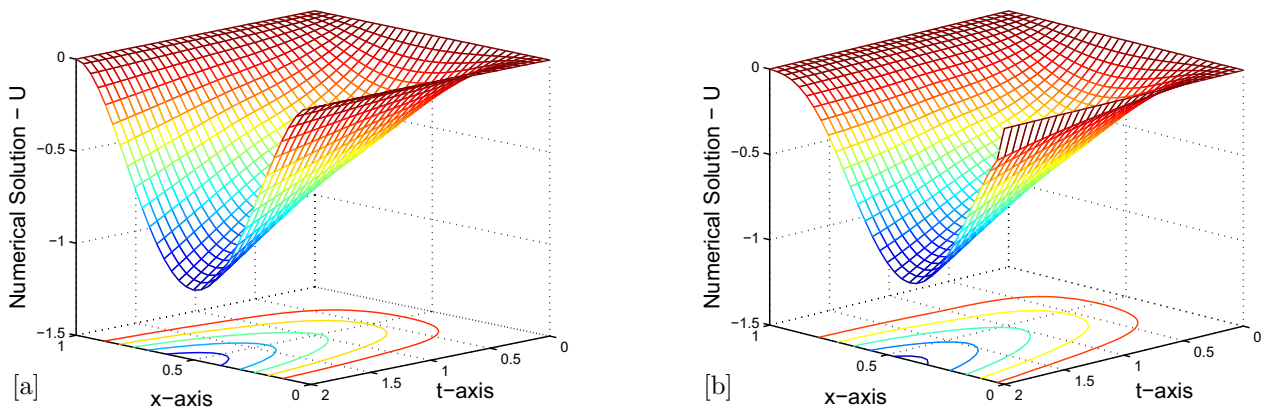


Fig. 1 Surface plot of the numerical solution for Example 1 with $N = M = 32$, (a) $\epsilon = 10^{-1}, \mu = 10^{-6}$ (b) $\epsilon = 10^{-6}, \mu = 10^{-1}$.

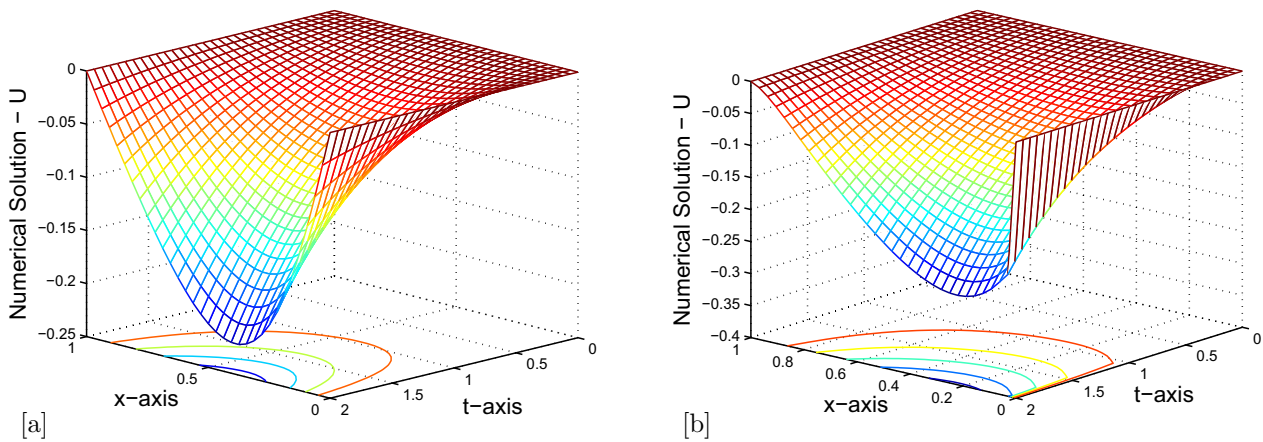


Fig. 2 Surface plot of the numerical solution for Example 2 with $N = M = 32$, (a) $\epsilon = 10^{-1}, \mu = 10^{-6}$ (b) $\epsilon = 10^{-6}, \mu = 10^{-1}$.

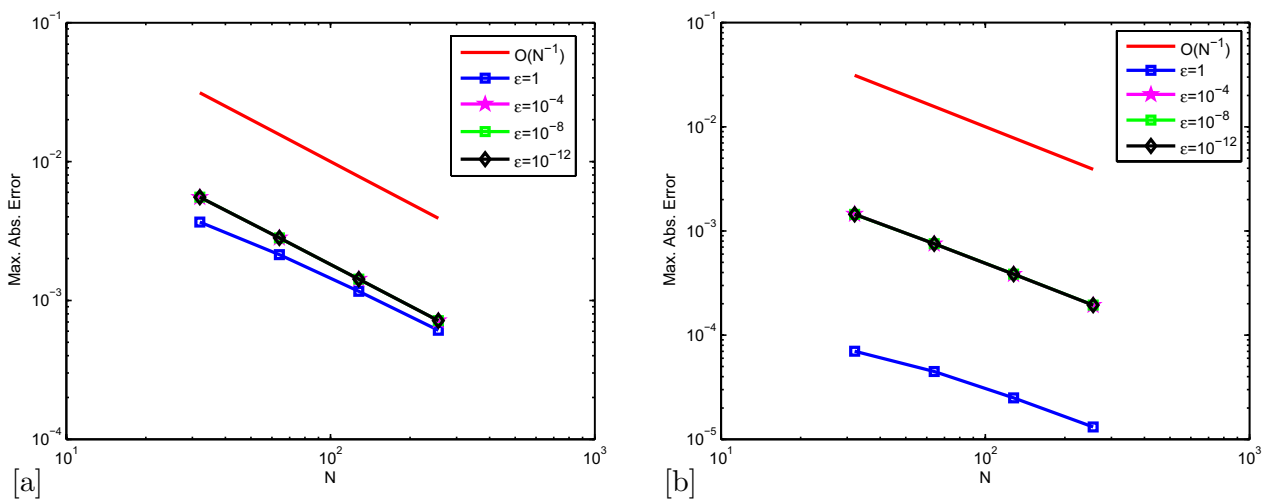


Fig. 3 Log-Log plot of the maximum error on left (a) for Example 1 with $\mu = 10^{-4}$ and on right (b) for Example 2 with $\mu = 10^{-4}$

first-order and second-order accurate uniformly convergent in time and space respectively. Two numerical tests are introduced to confirm the effectiveness of the proposed numerical scheme and approve the theoretical findings.

Limitations

The proposed uniformly convergent numerical approach is based on a uniform mesh that does not resolve boundary layers because there are not a sufficient number of mesh points in boundary regions.

Author contributions

The author read and approved the final manuscript.

Funding

No funding organization for this research work.

Availability of data and materials

No additional data is used for this research work.

Declarations

Ethics approval and consent to participate

Not applicable.

Consent for publication

Not applicable.

Competing interests

The author declares that he has no competing interests.

Received: 18 January 2023 Accepted: 10 August 2023

Published online: 19 October 2023

References

- Liu X, Zhou M, Ansari AH, Chakrabarti K, Abbas M, Rathour L. Coupled fixed point theorems with rational type contractive condition via c -class functions and inverse c -class functions. *Symmetry*. 2022;14(8):1663.
- Iqbal J, Mishra VN, Mir WA, Dar AH, Ishtyak M, Rathour L. Generalized resolvent operator involving (\cdot, \cdot) -co-monotone mapping for solving generalized variational inclusion problem. *Georgian Math J*. 2022;29(4):533–42.
- Gupta S, Rathour L. Approximating solutions of general class of variational inclusions involving generalized $i? j$ - $(hp, ?)$ - q -accretive mappings. *FILOMAT*. 2023;37(19):6255–75.
- Kumar A, Verma A, Rathour L, Mishra LN, Mishra VN. Convergence analysis of modified $szász$ operators associated with hermite polynomials. *Rendiconti del Circolo Matematico di Palermo Series*. 2023;2:1–15.
- KRASNIQI XZ, Mishra LN. On the power integrability with weight of double trigonometric series. *Adv Stud Contemp Math*. 2021;31(2):221–42.
- Pathak VK, Mishra LN. Application of fixed point theorem to solvability for non-linear fractional hadamard functional integral equations. *Mathematics*. 2022;10(14):2400.
- Mishra LN, Pathak VK, Baleanu D. Approximation of solutions for nonlinear functional integral equations. *Aims Math*. 2022;7(9):17486–506.
- Sundareswaran R, Vijayan S, Venkatesh S, Mishra LN, Broum S, et al. Failure analysis of pump piping system using dematel svn methodology. *Neutrosophic Sets Syst*. 2023;53(1):13.
- Mehra S, Rathour L, Mishra LN, et al. Complete orthogonally modular metric space and fixed point results for orthogonal generalized f -contraction mappings. *Adv Stud Euro-Tbilisi Mathl J*. 2023;16(2):115–36.
- Ma W-X. Nonlocal pt -symmetric integrable equations and related riemann-hilbert problems. *Partial Differ Equ Appl Math*. 2021;4: 100190.
- Ma W-X, Lee J-H. A transformed rational function method and exact solutions to the $3+ 1$ dimensional jimbo-miwa equation. *Chaos Solitons Fractals*. 2009;42(3):1356–63.
- Ma W-X. A polynomial conjecture connected with rogue waves in the kdv equation. *Partial Differ Equ Appl Math*. 2021;3: 100023.
- Hailu WS, Duressa GF. Accelerated parameter-uniform numerical method for singularly perturbed parabolic convection-diffusion problems with a large negative shift and integral boundary condition. *Results Appl Math*. 2023;18: 100364.
- Gobena WT, Duressa GF. An optimal fitted numerical scheme for solving singularly perturbed parabolic problems with large negative shift and integral boundary condition. *Results Control Optim*. 2022;9: 100172.
- Ladyzhenskaia OA, Solonnikov VA, Ural'tseva NN. Linear and quasi-linear equations of parabolic type. Rhode: American mathematical soc; 1968.
- Negero NT, Duressa GF. Uniform convergent solution of singularly perturbed parabolic differential equations with general temporal-lag. *Iran J Sci Technol Trans Sci*. 2022;46(2):507–24.
- Woldaregay MM, Duressa GF. Accurate numerical scheme for singularly perturbed parabolic delay differential equation. *BMC Res Notes*. 2021;14(1):1–6.
- Bhathawala P, Verma A. A two-parameter singular perturbation solution of one dimension flow through unsaturated porous media. *Appl Math*. 1975;43(5):380–4.
- Van Harten A, Schumacher J. On a class of partial functional differential equations arising in feed-back control theory. Amsterdam: Elsevier; 1978.
- Tikhonov AN, Samarskii AA. Equations of mathematical physics. Chelmsford: Courier Corporation; 2013.
- Gupta A, Kaushik A, Sharma M. A higher-order hybrid spline difference method on adaptive mesh for solving singularly perturbed parabolic reaction-diffusion problems with robin-boundary conditions. *Numer Methods Partial Differ Equ*. 2023;39(2):1220–50.
- Duressa GF, Debela HG. Numerical solution of singularly perturbed differential difference equations with mixed parameters. *J Math Model*. 2021;9(4):691–705.
- Gelu FW, Duressa GF. A parameter-uniform numerical method for singularly perturbed robin type parabolic convection-diffusion turning point problems. *Appl Numer Math*. 2023;190:50–64.
- Chandru M, Prabha T, Das P, Shanthi V. A numerical method for solving boundary and interior layers dominated parabolic problems with discontinuous convection coefficient and source terms. *Differ Equ Dyn Syst*. 2019;27(1):91–112.
- Kumar D. A parameter-uniform scheme for the parabolic singularly perturbed problem with a delay in time. *Numer Methods Partial Differ Equ*. 2021;37(1):626–42.
- Negero NT, Duressa GF. A method of line with improved accuracy for singularly perturbed parabolic convection-diffusion problems with large temporal lag. *Results Appl Math*. 2021;11: 100174.
- Negero N, Duressa G. An efficient numerical approach for singularly perturbed parabolic convection-diffusion problems with large time-lag. *J Math Model*. 2022;10(2):173.
- Negero NT, Duressa GF. An exponentially fitted spline method for singularly perturbed parabolic convection-diffusion problems with large time delay. *Tamkang Journal of Mathematics* 2022.
- Negero NT, Duressa GF. Parameter-uniform robust scheme for singularly perturbed parabolic convection-diffusion problems with large time-lag. *Comput Methods Differ Equ*. 2022;10(4):954–68.
- Negero NT. A robust fitted numerical scheme for singularly perturbed parabolic reaction-diffusion problems with a general time delay. *Results Phys*. 2023;51: 106724.
- Tesfaye SK, Woldaregay MM, Dinka TG, Duressa GF. Fitted computational method for solving singularly perturbed small time lag problem. *BMC Res Notes*. 2022;15(1):1–10.
- Li J, Navon IM. Uniformly convergent finite element methods for singularly perturbed elliptic boundary value problems i: reaction-diffusion type. *Comput Math Appl*. 1998;35(3):57–70.

33. Li J. Convergence analysis of finite element methods for singularly perturbed problems. *Comput Math Appl*. 2000;40(6–7):735–45.
34. Govindarao L, Mohapatra J, Sahu S. Uniformly convergent numerical method for singularly perturbed two parameter time delay parabolic problem. *Int J Appl Comput Math*. 2019;5(3):1–9.
35. Kumar S, Kumar M, et al. A robust numerical method for a two-parameter singularly perturbed time delay parabolic problem. *Comput Appl Math*. 2020;39(3):1–25.
36. Negero NT. A uniformly convergent numerical scheme for two parameters singularly perturbed parabolic convection-diffusion problems with a large temporal lag. *Results Appl Math*. 2022;16: 100338.
37. Negero NT. Fitted cubic spline in tension difference scheme for two-parameter singularly perturbed delay parabolic partial differential equations. *Partial Differ Equ Appl Math*. 2023. <https://doi.org/10.1016/j.padiff.2023.100530>.
38. Negero NT. A fitted operator method of line scheme for solving two-parameter singularly perturbed parabolic convection-diffusion problems with time delay. *J Math Model*. 2023. <https://doi.org/10.2212/JMM.2023.23001.2039>.
39. Negero NT. A parameter-uniform efficient numerical scheme for singularly perturbed time-delay parabolic problems with two small parameters. *Partial Differ Equ Appl Math*. 2023;7: 100518.
40. Negero N. A robust uniformly convergent scheme for two parameters singularly perturbed parabolic problems with time delay. *Iran J Numer Anal Optim*. 2023. <https://doi.org/10.2206/IJNAO.2023.80721.1214>.
41. Linß T, Roos H-G. Analysis of a finite-difference scheme for a singularly perturbed problem with two small parameters. *J Math Anal Appl*. 2004;289(2):355–66.
42. Hall C. On error bounds for spline interpolation. *J Approx Theory*. 1968;1(2):209–18.

Publisher's Note

Springer Nature remains neutral with regard to jurisdictional claims in published maps and institutional affiliations.

Ready to submit your research? Choose BMC and benefit from:

- fast, convenient online submission
- thorough peer review by experienced researchers in your field
- rapid publication on acceptance
- support for research data, including large and complex data types
- gold Open Access which fosters wider collaboration and increased citations
- maximum visibility for your research: over 100M website views per year

At BMC, research is always in progress.

Learn more biomedcentral.com/submissions

